

# Application of the Surface Complexation Concept to Complex Mineral Assemblages

J. A. DAVIS,\* J. A. COSTON,  
D. B. KENT, AND C. C. FULLER

U.S. Geological Survey, MS-465, 345 Middlefield Road,  
Menlo Park, California 94025

Two types of modeling approaches are illustrated for describing inorganic contaminant adsorption in aqueous environments: (a) the component additivity approach and (b) the generalized composite approach. Each approach is applied to simulate  $\text{Zn}^{2+}$  adsorption by a well-characterized sediment collected from an aquifer at Cape Cod, MA.  $\text{Zn}^{2+}$  adsorption by the sediment was studied in laboratory batch experiments with a range of pH and  $\text{Zn}(\text{II})$  concentrations selected to encompass conditions observed in the aquifer. In the generalized composite approach, one- and two-site surface complexation model parameters were calibrated with the experimental data using FITEQL. The pH dependence of  $\text{Zn}^{2+}$  adsorption was simulated without explicit representation of electrostatic energy terms. Surface acidity constants and ion pair formation by major electrolyte ions were also not required in the model, thereby minimizing the number of fitted parameters. Predictions of  $\text{Zn}^{2+}$  adsorption with the component additivity modeling approach did not simulate the experimental data adequately without manipulation of surface area or site density parameter values. To apply the component additivity approach to environmental sorbents, further research is needed to better characterize the composition of sediment surface coatings. The generalized composite modeling approach requires less information and can be viewed as more practical for application within solute transport models. With only three adjustable parameters, this approach could simulate  $\text{Zn}^{2+}$  adsorption over a range of chemical conditions that would cause several orders of magnitude variation in the distribution coefficient ( $K_d$ ) for  $\text{Zn}^{2+}$  within the aquifer.

## Introduction

Since publication of the seminal papers on the surface complexation (SC) concept by Professors Stumm and Schindler (1–4), a voluminous literature on ion adsorption and SC modeling has appeared. Although a number of variations in the modeling approach have been developed, there are four tenets of all SC models (5):

(a) The mineral surface is composed of specific functional groups that react with dissolved solutes to form surface species (coordination complexes or ion pairs), in a manner analogous to complexation reactions in homogeneous solution.

(b) The equilibria of SC and surface acidity reactions can be described by mass action equations. If desired, correction

factors to these equations may be applied to account for variable electrostatic energy, using electrical double-layer theory.

(c) The apparent binding constants determined for the mass action equations are empirical parameters related to thermodynamic constants by the rational activity coefficients of the surface species (6).

(d) The electrical charge at the surface is determined by the chemical reactions of the mineral functional groups, including acid–base reactions and the formation of ion pairs and coordinative complexes.

The literature on SC modeling largely describes the results of well-controlled laboratory investigations of the adsorption of ions by a variety of mineral phases. Most of these studies have been undertaken by aquatic scientists interested in developing a thermodynamic understanding of the coordinative properties of mineral surface functional groups. Applications of the SC concept to adsorption of ions by soils and sediments are relatively rare due to the complexity of natural systems. Some notable examples include the work of Zachara and colleagues (7–11) and a few other investigators (e.g., refs 12–14). One of the complexities of soils and sediments is identifying the mineralogical composition in the near-surface region of sediment grains (15). In addition, the composition of aqueous solutions is not easily controlled in experiments with soils and sediments. This condition makes it more difficult to determine “intrinsic” stability constants of molecular scale reactions for sediment surfaces than is the case for single mineral phases bathed in simple electrolyte solutions.

The quantification of Coulombic correction factors for the electrical double layer on the surfaces of particles is equally complex. Interacting double layers of heterogeneous particles (16), the formation of surface coatings (17, 18), and the competitive adsorption of many different ions (19) cause significant changes in the electrical properties of mineral–water interfaces. As a result, the surface charge and electrical potential of the surfaces of soils and sediments are much more difficult to quantify than is the case for the pure mineral phases commonly used in laboratory investigations. For example, the surface charge of hydrous oxide phases is typically determined by potentiometric titrations of oxide suspensions (1–5, 20, 21). The analysis and interpretation of such titration data is made by assuming that all protons consumed or released by the solid phase (corrected for solid-phase dissolution) are due to acid–base reactions of the surface functional groups. However, this assumption usually cannot be justified when soil or sediment suspensions are titrated (22), and the analysis and interpretation of such data are extremely complex due to dissolution of poorly crystalline phases and desorption of solutes, such as fulvic acids.

To develop an SC model, the following steps must be taken:

(a) The total number of surface sites (functional groups) must be determined experimentally or a value must be assigned from other studies.

(b) An approach must be developed to describe surface site heterogeneity or the number of specific types of surface sites.

(c) The mass action and mass balance equations that describe the equilibria of surface reactions must be formulated, and the apparent stability constants for surface species must be determined.

(d) An approach must be developed or assumed to quantify Coulombic correction factors or rational activity

\* Corresponding author telephone: (650)329-4484; fax: (650)-329-4327; e-mail: jadavis@usgs.gov.

TABLE 1. Characteristics of SC Modeling Approaches for Environmental Sorbents

component additivity	generalized composite
predict adsorption	simulate adsorption
surface sites are unique for each specific sorbent	generic surface sites
surface site densities quantified by characterization of the surface of the environmental sorbent mixture	surface site densities quantified by measurement of surface area and fitting of experimental data for the environmental sorbent mixture
apparent stability constants and reaction stoichiometries obtained from studies of adsorption by specific sorbents	apparent stability constants and reaction stoichiometries fit to experimental data for the environmental sorbent mixture
overall adsorption predicted by sum of adsorption by each specific sorbent	numbers of site types and chemical reactions increased as necessary to achieve good model simulations and to meet modeling objectives

coefficients to correct the equilibrium constants of surface acidity and complexation reactions.

In this paper we describe some potential approaches for applying the SC concept to model trace ion adsorption to soils and sediments, using  $\text{Zn}^{2+}$  adsorption by an aquifer sediment as an example. The modeling approaches can be subdivided into two major types: (a) the *component additivity* approach and (b) the *generalized composite* approach (Table 1). In the component additivity (CA) approach, the modeler attempts to *predict* adsorption on a complex mineral assemblage, using the results of a surface characterization of the assemblage and collected data for adsorption by pure, reference minerals or organic phases (10, 14, 23–26). Strictly speaking, no fitting of data is required to develop the model for the mixed mineral assemblage in the CA approach, although comparisons of model simulations and experimental adsorption data for the assemblage are needed to build confidence in the model (25, 26). It is assumed in this approach that the wetted surface of the complex mineral assemblage is composed of a mixture of one or more mineral (or organic) phases whose surface properties are known from independent studies of the individual phases. From the studies of individual phases, a database of internally consistent SC equilibria can be developed that describe the adsorption reactions of solutes to each phase. For example, the compilation of Dzombak and Morel (20) for hydrous ferric oxide represents such a database for an important adsorbing phase, and other databases are currently being developed (27). Once the relative abundance and identity of the major adsorptive phases have been determined and the appropriate databases for reference mineral phases have been assembled, a system of mass law equations can be written to describe the SC equilibria for each phase of the mixture.

In the generalized composite (GC) approach, it is assumed that the surface composition of the mineral assemblage is inherently too complex to be quantified in terms of the contributions of individual phases to adsorption. Instead, it is assumed that the adsorptive reactivity of the surface can be described by SC equilibria written with “generic” surface functional groups, with the stoichiometry and formation constants for each SC equilibria determined by fitting experimental data (12, 14, 28, 29). This approach can also be simplified by fitting the pH dependence of adsorption without explicit representation of electrostatic energies. Examples of these two major types of SC modeling approaches are presented below.

## Materials and Methods

Adsorption experiments were conducted with sediments collected at the U.S. Geological Survey research site in Falmouth, MA, on Cape Cod. The study site is a shallow, unconfined aquifer of unconsolidated glacial outwash sands and gravels (30). Sediments in the aquifer consist predomi-

nantly of a medium to coarse sand. The sand mineralogy is dominated by quartz and feldspars; Fe-bearing accessory minerals are present in low abundances (17). Carbonate minerals were absent from the aquifer material. Organic carbon content in the sediments is low, ranging from 0.01 to 0.05 wt %, and the combined silt and clay sized material comprises less than 1 wt % (31).

Sand grains examined by optical microscopy and SEM showed evidence of chemical and mechanical weathering. Quartz grains are covered with a coating rich in Al, Fe, and Si (17, 32). Thick coatings ( $>5\ \mu\text{m}$ , detected by SEM) exhibited a patchy distribution on the surface, but thin coatings (10–30 nm, detected by TOF–SIMS) appeared to cover the entire surface of quartz grains (17).

Batch adsorption experiments were conducted with a composite sample of sediment prepared from several cores collected at the site and described in detail by Coston et al. (17). The composite sediment sample had a BET surface area of  $0.44\ \text{m}^2/\text{g}$ . The experiments were conducted in an artificial groundwater (AGW) solution that approximated the typical major ion composition of groundwater collected from the suboxic zone of the aquifer (17, 33). All batch experiments were performed according to the experimental protocol described in Coston et al. (17) as the  $\text{CO}_2$ -buffered method of pH adjustment, except for a few batch experiments performed for comparison with the pH buffer, 2-(*N*-morpholino)ethanesulfonic acid (MES). MES is a zwitterionic amino acid buffer that has been used in other studies of metal ion sorption and dissolution (34). Dried composite sediment was washed with AGW for 2 h prior to batch adsorption experiments and then by two 2-h washes of AGW containing 0.05 M added MES or equilibrated with a gas mixture of  $\text{N}_2$ ,  $\text{O}_2$ , and  $\text{CO}_2$  (the partial pressure of  $\text{CO}_2$  was a variable used to achieve different final pH values).  $\text{Zn}^{2+}$  was added to the experiments from freshly prepared, unacidified 2 mM  $\text{Zn}(\text{NO}_3)_2$  stock solutions, and the sediment suspension was mixed for 48 h. This methodology avoided the problems of Al dissolution and reprecipitation encountered in the pH-drift experiments described by Coston et al. (17). The  $\text{CO}_2$ -buffered protocol resulted in pH drifts less than 0.2 pH unit during the experiments; the MES-buffered systems had drifts less than 0.05 pH unit. Other details of the experimental and analytical procedures are given in Coston et al. (17).

The data set used to develop the SC models described in this paper is comprised primarily of new data collected for this study, but the data set also includes  $\text{Zn}^{2+}$  adsorption data (five experimental points) from Coston et al. (17) that were determined with the  $\text{CO}_2$ -buffered method of pH adjustment. Batch adsorption experiments were performed over the pH range 4.90–7.37, with total zinc concentrations ranging from  $1.7 \times 10^{-7}$  to  $1.0 \times 10^{-4}$  M and with sediment/water ratios of 400 and 50 g/L, respectively (corresponding to surface areas of 176 and  $22\ \text{m}^2/\text{L}$ ).

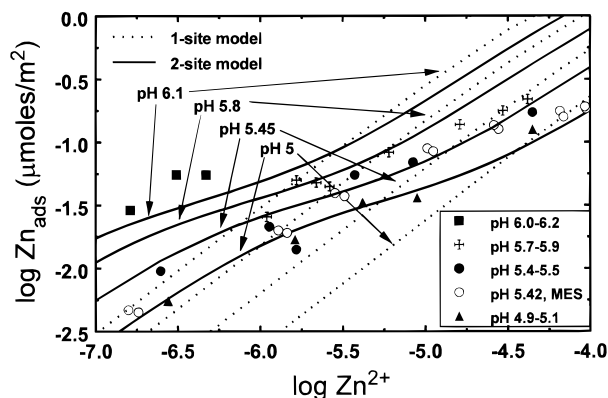


FIGURE 1.  $\text{Zn}^{2+}$  adsorption density ( $\mu\text{mol}/\text{m}^2$ ) on the Cape Cod sediment in AGW solution as a function of aqueous  $\text{Zn}^{2+}$  concentration for selected pH ranges. In the pH range 5.4–5.5, data are compared for AGW solutions buffered with  $\text{CO}_2(\text{g})$  or MES. Dotted (one site—one proton model) and solid curves (two site—one proton model) illustrate FITEQL fits to all of the experimental data in  $\text{CO}_2$ -buffered systems at pH values in the mid-pH range of the experimental data.

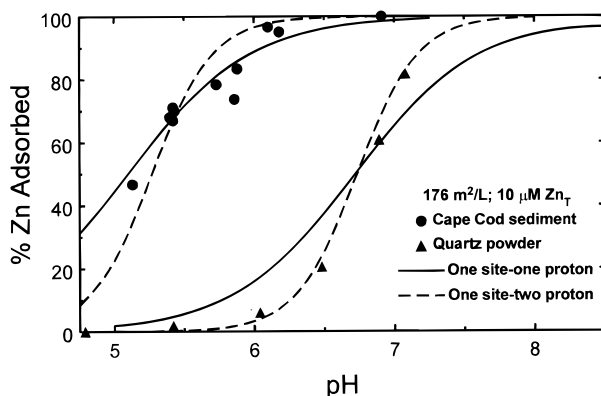


FIGURE 2.  $\text{Zn}^{2+}$  adsorption as a function of pH on Cape Cod sediment and purified quartz powder at a total  $\text{Zn}(\text{II})$  concentration of  $10^{-5}$  M and with surface areas of  $176 \text{ m}^2/\text{L}$ . Solid curves illustrate FITEQL fits to these experimental data with the one site—one proton model. Dashed curves illustrate FITEQL fits to these experimental data with the one site—two proton model. Quartz data are from Coston et al. (17).

The experimental conditions were chosen to match the field conditions in a region of the aquifer at Cape Cod that is contaminated with adsorbed and dissolved Zn (35, 36). In particular, the experiments were designed to achieve a wide range of Zn adsorption densities on the surface of the sediment, such that the range was greater than that observed in the aquifer. A total of 50 batch experiments were performed, but because of the varied chemical conditions, not all data are shown in the figures.

## Experimental Results

Figure 1 shows Zn adsorption isotherms for the Cape Cod sediment at four pH values, with Zn adsorption density plotted as a function of the equilibrium aqueous concentration of  $\text{Zn}^{2+}$ . The equilibrium aqueous concentration of  $\text{Zn}^{2+}$  was computed with HYDRAQL (37) from the measurement of total dissolved Zn in the batch experiments. Aqueous  $\text{Zn}(\text{II})$  speciation in AGW and in the aquifer is dominated by  $\text{Zn}^{2+}$  (94% of dissolved Zn) and  $\text{ZnSO}_4^0(\text{aq})$  (17). The isotherms have a slope of about 0.6 when plotted on a log–log scale (Figure 1), similar to the slopes observed for adsorption of many cations on hydrous metal oxides (5, 38, 39). Sixteen batch experiments were conducted in the presence of MES buffer at pH 5.4, and the results of these

experiments compared extremely well with those in the same pH range without MES buffer (Figure 1).

When plotted as fraction (or percent) adsorbed, the data for  $\text{Zn}^{2+}$  adsorption on the composite sediment sample show less dependence on pH than that typically found for pure hydrous oxide surfaces. This can be seen by comparing  $\text{Zn}^{2+}$  adsorption data on the Cape Cod sediment with that observed for purified quartz powder under identical chemical conditions (Figure 2). The characteristic “adsorption edge”, where adsorption rises from near zero to nearly complete adsorption, encompasses a smaller pH range on the quartz powder (1.5 pH units) than on the Cape Cod sediment. This weaker dependence of cation adsorption on pH for the sediment sample is believed to be due to a greater heterogeneity of surface functional groups in the complex mineral assemblages of soils and sediments (5, 40), including the possible influence of organic and phosphato ligands present at the sediment surfaces.

## SC Modeling Approaches for Complex Mineral Assemblages

The surface properties of mineral phases in soil and subsurface environments are greatly altered by the accumulation of poorly crystalline phases of iron(III) and aluminum oxyhydroxides and silicates (15). Diagenesis and interactions with bacteria may cause leaching of surface layers of minerals (41), formation of various mixed layer clays, and deposition of extremely fine-grained, high surface area precipitates (42). For SC modeling, the principal difficulties posed by these materials are that the identity, structure, composition, and electrical double-layer properties of the wetted surface are usually not well known. As will be discussed below, this fact has important ramifications for the approach to SC modeling, as some of the a priori assumptions and experimental techniques that are used in developing an SC model for a pure, single mineral phase may not be valid for developing an SC model for a complex mineral assemblage.

In many cases, the surface chemical properties of sediments may be completely dominated by secondary minerals or grain coatings, which usually constitute only a minor fraction of the sediment mass (17, 43, 44). It has been shown that the surfaces of silica, rutile, ferrihydrite, and goethite become enriched with Al when they are mixed with poorly crystalline alumina phases or solutions containing dissolved Al (19, 45). These types of surface enrichment can greatly alter the chemical and adsorptive properties of mineral surfaces (18, 46). Thus, the observation that the quartz powder surface is less reactive than the Cape Cod sediment surface (Figure 2) is not surprising, because of the extensive Al- and Fe-rich surface coatings identified on quartz grains in the sediment (17).

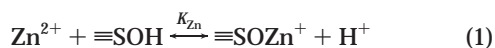
**Determination of Total Surface Site Density for Complex Mineral Assemblages.** For a single mineral phase, the total site density can be determined experimentally by a variety of methods or calculated from an analysis of the densities of surface functional groups on the exposed crystal and cleavage faces of a mineral (5). Some of the techniques cannot be as easily applied to soils or sediments to determine surface site density because of experimental interferences. As mentioned above, the interpretation of acid–base potentiometric titrations is very difficult due to other interfering reactions (22). It is usually not possible to determine the total site density directly by adsorption of metal ions, because polymerized surface species may form at high adsorption densities (47) and the solubility of an oxide or carbonate phase is often reached in experiments before surface sites are saturated. Other methods, such as the tritium exchange method (48), have not been adequately tested with soils and sediments.



For a complex mineral assemblage, the most expedient approach for determining total surface site density for SC modeling is to carefully measure the "reactive" specific surface area of the assemblage. The reactive surface area of a sample depends on its composition and the nature of the adsorption reactions under consideration. For example, the basal planes of 2:1 layered aluminosilicate minerals are considered unreactive for some SC equilibria (49, 50), and the modeler may want to exclude the surface area of these faces from the SC model. In this case, the BET surface area of the sample may be the best experimental determination of the reactive surface area (5). However, for certain poorly crystalline structures that contain significant water, e.g., ferrihydrite or imogolite, the reactive surface area may be larger than what is determined by the BET method (51), and the surface area may need to be assumed based on values found in the literature for these poorly crystalline phases.

Once the specific surface area has been determined, one can quantify the surface concentration of functional groups that participate in SC equilibria from measurements of the site density of single mineral phases. The site densities of many mineral phases per unit surface area are available in the literature (5). In the CA modeling approach, the surface area of each mineral phase present at the surface can be multiplied by the site density of that phase. For the GC approach, the recommended site density is 3.84  $\mu\text{mol}$  of surface sites per square meter of surface area (5), which was chosen to be consistent with the value recommended by others for ferrihydrite (20).

**Electrostatic Correction Terms for Surface Complexation Equilibria.** Several SC models with different approaches for correcting mass action equations for Coulombic effects have been proposed (5). In the diffuse double-layer (DDL) model of Dzombak and Morel (20), the molecular scale reaction that describes the adsorption of  $\text{Zn}^{2+}$  by iron oxides is



where  $\equiv\text{SOH}$  refers to a structurally undefined, average functional group on the surface (assumed to be an amphoteric hydroxyl group), and  $K_{\text{Zn}}$  is the "intrinsic" stability constant for the mass action equation. Equation 1 suggests that one proton is released per  $\text{Zn}^{2+}$  adsorbed at the surface; however, the increased surface charge and potential that result from the formation of the surface complex promote additional proton release through Coulombic repulsion. With correction to eq 1 for Coulombic effects, calculations with the DDL model suggest that 1.7–2.0 protons are released per  $\text{Zn}^{2+}$  adsorbed on ferrihydrite, depending on the pH and ionic strength of the solution (20). This result is in good agreement with the experimental study of Kinniburgh (52), who measured a macroscopic release of 1.7 protons released per  $\text{Zn}^{2+}$  adsorbed on an iron oxide surface at high ionic strength ( $\approx 1 \text{ M}$ ).

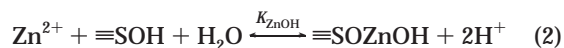
Perhaps the simplest of all SC models is the nonelectrostatic model (NEM), which considers surface equilibria strictly as chemical reactions, without explicit correction for electrostatic attraction or repulsion (53). In the NEM, the pH-dependent Coulombic energy contribution to the mass action equation is simply included within the apparent binding constant. The apparent binding constants and the stoichiometry of the mass action equations are derived by fitting the *macroscopic* dependence of ion adsorption as a function of pH, as will be shown below. As a result, the mass action equations that describe ion adsorption in an NEM are not expected to provide accurate representations of the stoichiometry of the reactions at the molecular scale.

While it has been applied in relatively few instances (8, 10, 29, 54), the NEM may be the most appropriate for

environmental applications because of its simplicity. Since it is difficult to assess the actual surface charge of mineral phases in complex mixtures of phases (16, 22), it will usually not be possible to apply the appropriate electrostatic correction terms that are required in the more complex SC models, such as the DDL or triple-layer model (TLM; 21). It is known that the surface charge of mineral phases in natural waters is very different from that observed in simple electrolyte solutions. For example, the adsorption of some major ions in natural waters (e.g.,  $\text{Mg}^{2+}$ ,  $\text{Ca}^{2+}$ ,  $\text{SO}_4^{2-}$ , and silicate) and the formation of organic coatings are known to cause large changes in measurements of the point-of-zero-charge ( $\text{pH}_{\text{PZC}}$ ) and isoelectric point ( $\text{pH}_{\text{IEP}}$ ) of mineral phases (5, 18, 22, 55). Charlet and Sposito (56) have proposed an elegant experimental method for determining the electrical double-layer properties of composite materials, but this method has not yet been widely applied.

### Generalized Composite Modeling Approach

While the GC modeling approach can be used with electrostatic correction terms (12), we have chosen to use the NEM for the calculations illustrating this approach. The average free energy of complexation of  $\text{Zn}^{2+}$  with surface sites on the Cape Cod composite sediment can be characterized with the NEM by assuming that all surface sites in the sample are chemically equivalent (referred to as a one-site model). To apply the model, integral stoichiometries are proposed for the simplest and most chemically plausible surface equilibria, and apparent stability constants are derived by fitting experimental data. For example, adsorption of  $\text{Zn}^{2+}$  by the Cape Cod sediment might be described by eq 1 above plus the following reaction:



where  $K_{\text{ZnOH}}$  is the apparent stability constants for the mass action equation. Alternatively, eq 2 could be written as a reaction between  $\text{Zn}^{2+}$  and two adjacent surface sites, each releasing one proton (4, 57, 58). For the Cape Cod sediment sample, a total surface site density of 1.69  $\mu\text{mol}$  of surface sites/g of sediment was used for SC modeling, based on the surface area of 0.44  $\text{m}^2/\text{g}$  and the assumed site density of 3.84  $\mu\text{mol}$  of surface sites/ $\text{m}^2$  (5). Values for  $K_{\text{Zn}}$  and  $K_{\text{ZnOH}}$  were estimated by fitting experimental data with the computer program FITEQL (59). Different reaction stoichiometries or model formulations can be compared with the goodness-of-fit parameter (SOS/DF), which is an output of the FITEQL computations.

Model simulations of a portion of the experimental data for  $\text{Zn}^{2+}$  adsorption by the Cape Cod sediment and the quartz powder are shown in Figure 2. Simulations using only eq 1 are referred to as the one site—one proton model, and those using only eq 2 are referred to as the one site—two proton model. The apparent stability constants are given in Table 2. As mentioned previously, the experimental data show that the pH dependence of  $\text{Zn}^{2+}$  adsorption on the Cape Cod sediment is less steep than that observed in studies of hydrous oxides, and the modeling results confirm this observation. Using only one reaction,  $\text{Zn}^{2+}$  adsorption by the sediment is best fit with eq 1, while the best fit to the quartz data is with eq 2. In each case though, the pH dependence of  $\text{Zn}^{2+}$  adsorption was reasonably well described with only one surface reaction. Comparing the apparent constants for the one site—one proton models for quartz and the composite sediment (Table 2) shows that the "average" sediment surface site was about 1.5 orders of magnitude more reactive than the purified quartz powder surface.

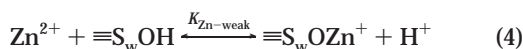
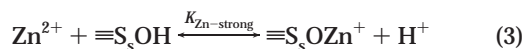
**Fitting Adsorption Isotherms with the GC Modeling Approach.** While the one site—one proton model fit the experimental data well at a single Zn concentration

TABLE 2. Parameters Used in Surface Complexation Models

mineral	stability constant	site density	figure	model type
Cape Cod sediment	$\log K_{Zn} = -2.20^d$	$3.84 \mu\text{mol}/\text{m}^2$	1	one site—one proton
Cape Cod sediment	$\log K_{Zn\text{--strong}} = 0.85^e$	$0.033 \mu\text{mol}/\text{m}^2$	1	two site—one proton
	$\log K_{Zn\text{--weak}} = -2.40$	$3.81 \mu\text{mol}/\text{m}^2$		
Cape Cod sediment	$\log K_{Zn} = -1.90^a$	$3.84 \mu\text{mol}/\text{m}^2$	2	one site—one proton
Cape Cod sediment	$\log K_{ZnOH} = -7.34^b$	$3.84 \mu\text{mol}/\text{m}^2$	2	one site—two proton
quartz	$\log K_{Zn} = -3.50^c$	$3.84 \mu\text{mol}/\text{m}^2$	2	one site—one proton
quartz	$\log K_{ZnOH} = -10.2^c$	$3.84 \mu\text{mol}/\text{m}^2$	2	one site—two proton
goethite <sup>f</sup>	$\log K_{Zn} = -2.59^g$	$3.84 \mu\text{mol}/\text{m}^2$	6	one site—one proton
poorly crystalline alumina	$\log K_{Zn} = -2.94^h$	0.205 mol of sites/mol of Al	6	one site—one proton
ferrihydrite	$\log K_{Zn} = -2.59^i$	0.205 mol of sites/mol of Fe	6	one site—one proton

<sup>a</sup> Fit to data in Figure 2 only with FITEQL; SOS/DF = 5.1. <sup>b</sup> Fit to data in Figure 2 only with FITEQL; SOS/DF = 20.0. <sup>c</sup> Fit to data in Figure 2 only with FITEQL. <sup>d</sup> Fit to all experimental data for CO<sub>2</sub>-equilibrated batch experiments; SOS/DF = 17.0. <sup>e</sup> Fit to all experimental data for CO<sub>2</sub>-equilibrated batch experiments; SOS/DF = 6.4. <sup>f</sup> Goethite in Cape Cod sediment surface coating assumed to have a surface area of 50 m<sup>2</sup>/g. <sup>g</sup> Fit to experimental data of McKenzie (69) with FITEQL. <sup>h</sup> Fit to experimental data of Kinniburgh and Jackson (70) with FITEQL, assuming a surface area of 111 m<sup>2</sup>/g for the alumina in their batch experiments. Surface area estimate from McBride (77). <sup>i</sup> Fit to experimental data of Dempsey and Singer (77) with FITEQL, assuming a site density of 0.205 mol of surface sites/mol of Fe, as recommended by Dzombak and Morel (20).

(Figure 2), this simple model did not fit adsorption isotherms well when fit to the complete Zn<sup>2+</sup> adsorption data set (Figure 1). With a one site model, the predicted isotherm is a Langmuir isotherm, with a slope of 1 on a log–log scale at low adsorption densities. The Zn adsorption isotherms have a slope of 0.6 on a log–log scale, and the data can be fitted better with a multiple-site Langmuir expression or the Freundlich isotherm (5). Most adsorption data can usually be modeled with an assumption of two nonequivalent sites (60), and this approach was chosen here to keep the model simple. Following the terminology of Dzombak and Morel (20), we shall refer to the generic sites as “strong” and “weak” sites, and the model is referred to as a two site model. Given the good fit of eq 1 to the experimental data at a single Zn concentration, we next propose a model to describe the complete Zn<sup>2+</sup> adsorption data set using two reactions with the same stoichiometry



where  $\equiv\text{S}_s\text{OH}$  and  $\equiv\text{S}_w\text{OH}$  refer to the strong and weak surface sites, respectively, and  $K_{Zn\text{--strong}}$  and  $K_{Zn\text{--weak}}$  are the apparent stability constants. The total site density used for the two site model was the same as in the one site model calculations. The strong site density for the two site model was determined by iterative computations with FITEQL to find the value of the strong site density that gave the best fit to the experimental data (Figure 3). The value found was a strong site density equal to 0.86% of the total sites, corresponding to a strong site density of  $0.033 \mu\text{mol}/\text{m}^2$  of sediment surface area and a weak site density of  $3.81 \mu\text{mol}/\text{m}^2$ . The stability constants,  $K_{Zn\text{--strong}}$  and  $K_{Zn\text{--weak}}$ , at these site densities were determined with FITEQL by the best fit to the experimental data (Table 2). Waite et al. (61) reported a strong site density on ferrihydrite of  $0.034 \mu\text{mol}/\text{m}^2$  in a study of U(VI) adsorption, very similar to the value for strong site density found for the Cape Cod sediment.

The fit of the two site—one proton model to the Zn adsorption isotherm data is shown in Figure 1. While the fit is not perfect, it is clearly a large improvement over the one site model because of the change in slope of the predicted isotherms. The curvature in the calculated isotherms for the two site model is the result of the summation of separate Langmuir isotherms for each site type. The curvature in the isotherms is observed near the value of the strong site density ( $\log = -1.48 \mu\text{mol}/\text{m}^2$ ), as Zn<sup>2+</sup> adsorption nears saturation on these sites (Figure 1). The aqueous Zn<sup>2+</sup> concentration at which this occurs depends on the pH.

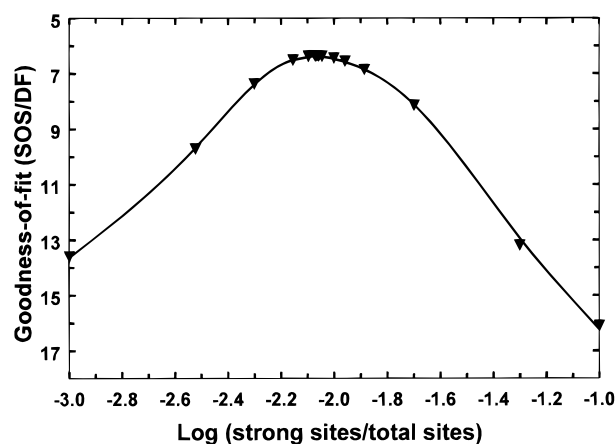


FIGURE 3. Variation of the FITEQL goodness-of-fit parameter with the ratio of strong sites/total sites in fits of the two site—one proton model to all of the experimental data for Zn<sup>2+</sup> adsorption on Cape Cod sediment in CO<sub>2</sub>-buffered systems.

Figures 4 and 5 compare the simulations of the one site and two site models with experimental data at several different Zn concentrations for batch experiments containing 176 and 22 m<sup>2</sup>/L of suspended sediment. Both models fit the experimental data well in the experiments at high Zn concentrations, but the two site model performs better at lower Zn concentrations.

**Acid–Base Reactions of Surface Functional Groups.** The GC modeling calculations above were performed without including any reactions to describe the acid–base chemistry of the functional groups on the sediment surfaces (other than the release of protons due to Zn<sup>2+</sup> adsorption). As long as accurate values are chosen for the total surface site density (2–10 sites/nm<sup>2</sup>), surface site speciation is dominated by the uncharged surface species,  $\equiv\text{SOH}$ , over a wide range of pH and ionic strength in SC models that include acid–base reactions and corrections to mass action equations for Coulombic effects (20, 21). Thus, at low Zn<sup>2+</sup> adsorption densities, the concentration of  $\equiv\text{SOH}$  species is nearly constant and the formation  $\equiv\text{SOH}_2^+$  and  $\equiv\text{SO}^-$  can be neglected in the mass balance for surface sites, thereby reducing the number of fitted parameters in the model. The slight decrease in  $\equiv\text{SOH}$  concentration that does occur with pH is included by fitting the macroscopic dependence of Zn<sup>2+</sup> adsorption as a function of pH. When modeling very acidic or alkaline environments, the concentration of the uncharged surface species,  $\equiv\text{SOH}$ , may decrease significantly due to acid–base reactions. Under these conditions, it may

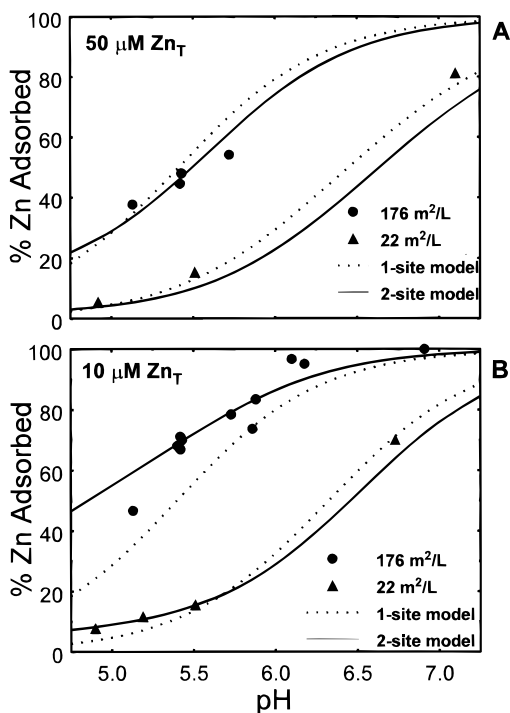


FIGURE 4.  $\text{Zn}^{2+}$  adsorption as a function of pH on Cape Cod sediment at surface areas of 176 and 22  $\text{m}^2/\text{L}$ . Dotted curves illustrate simulations of the one site—one proton model; solid curves illustrate simulations of the two site—one proton model. Both models were calibrated with all of the experimental data in  $\text{CO}_2$ -buffered systems. (A) total  $\text{Zn(II)}$  concentration of  $5 \times 10^{-5}\text{M}$ ; (B) total  $\text{Zn(II)}$  concentration of  $10^{-5}\text{M}$ .

be necessary to abandon the NEM modeling approach in favor of the DDL or TLM.

Westall et al. (28) have proposed a GC modeling approach for humic substances and surfaces of environmental solids that is similar to the one proposed here, except that these authors defined four site types, each with a model-imposed acidity constant. Site densities were determined mathematically by fitting potentiometric titration data. The results presented here, however, indicate that the GC modeling approach need not include acidity constants for surface sites in order to successfully describe experimental data as a function of pH. In addition, since the ionic strength dependence of adsorption of strongly binding cations is frequently negligible (5, 20), binding constants for univalent major electrolyte ions can often be omitted from the model. Competitive adsorption of  $\text{Ca}^{2+}$ ,  $\text{Mg}^{2+}$ , and other divalent major ions can be important (23, 62), and binding constants for these ions may need to be included *if their concentration varies* in the modeling application of interest. Thus, the number of reactions considered and fitting parameters introduced is influenced by the range of chemical conditions that must be modeled in an application. Clearly, a GC model should not be expected to perform well when simulations extrapolate beyond the chemical conditions for which the model was calibrated.

### Component Additivity Modeling Approach

Determining the identity and relative abundance of the major adsorptive phases is the greatest problem in applying the SC concept to complex mineral assemblages by the CA approach. Experimental techniques for quantifying the relative abundances of various surface functional groups in complex mineral assemblages are not well developed. Many investigators have relied on significant assumptions, such as the following: (1) the relative abundance of surface functional groups is proportional to the bulk mineralogical composition,

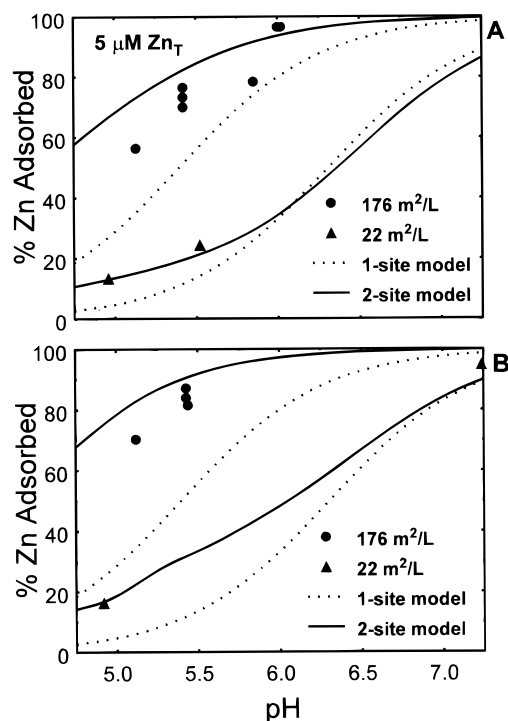


FIGURE 5.  $\text{Zn}^{2+}$  adsorption as a function of pH on Cape Cod sediment at surface areas of 176 and 22  $\text{m}^2/\text{L}$ . Dotted curves illustrate simulations of the one site—one proton model; solid curves illustrate simulations of the two site—one proton model. Both models were calibrated with all of the experimental data in  $\text{CO}_2$ -buffered systems. (A) total  $\text{Zn(II)}$  concentration of  $5 \times 10^{-6}\text{M}$ ; (B) 176  $\text{m}^2/\text{L}$ , total  $\text{Zn(II)}$  concentration of  $1 \times 10^{-6}\text{M}$ ; 22  $\text{m}^2/\text{L}$ , total  $\text{Zn(II)}$  concentration of  $2 \times 10^{-6}\text{M}$ .

as determined by X-ray diffraction, or (2) the adsorptive reactivity of the mineral assemblage is dominated by one specific mineral phase, such as ferrihydrite (40, 63). The quartz example above illustrates how the bulk mineralogy should not be equated with the surface composition for modeling purposes. The Cape Cod sediment is 95% quartz by weight, and  $\text{Zn}^{2+}$  adsorption occurs primarily on the quartz grains, but quartz powder is clearly not a good reference surface for CA modeling because  $\text{Zn}^{2+}$  adsorption is too weak (Figure 2). An assessment of the predominant adsorbing surface in a mineral assemblage, however, can be a useful approach if proven experimentally. For example, Fuller and Davis (64) showed that the sorption of  $\text{Cd}^{2+}$  by an aquifer sand was dominated by surface reactions with calcite grains. Using an NEM model, an apparent stability constant for the adsorption reaction of  $\text{Cd}^{2+}$  on pure calcite was determined (65), and it was observed that the constant could be applied to *predict* rapid  $\text{Cd}^{2+}$  adsorption by the aquifer sand without additional fitting.

It may not always be possible to identify a particular type of surface functional group that dominates adsorptive interactions. For example, Zachara et al. (66) showed that ferrinol and aluminol groups were both important in modeling  $\text{Cr(VI)}$  adsorption by a soil composed primarily of clay minerals, micas, and hydrous oxides. Turner et al. (7) argued that aluminol and silanol sites were the major surface reactants for  $\text{U(VI)}$  adsorption by a clay-sized subsurface mineral isolate, composed primarily of ferrogenuous beidellite. Zachara et al. (10) showed that  $\text{Co}^{2+}$  sorption by a clay-sized ultisol saprolite with sorbed humic acid was due to ferrinol, aluminol, and humic acid functional groups.

**Surface Functional Groups of the Cape Cod Sediment.** SIMS and Auger spectroscopy and aqueous extractions showed that quartz grains in the Cape Cod sediment were



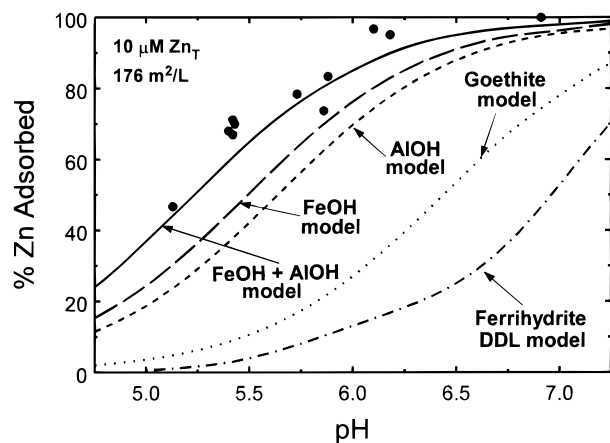


FIGURE 6.  $\text{Zn}^{2+}$  adsorption as a function of pH on Cape Cod sediment at a total  $\text{Zn(II)}$  concentration of  $10^{-5}\text{M}$  and with surface area of  $176\text{ m}^2/\text{L}$ . Dot-dash curve represents a simulation of  $\text{Zn}^{2+}$  adsorption by the ferrihydrite component of the Cape Cod sediment using the two site-one proton DDL model of Dzombak and Morel (20). Ferrihydrite component concentration estimated by 30-min HH extraction. Other curves represent simulations of  $\text{Zn}^{2+}$  adsorption by various components of the Cape Cod sediment using a one site-one proton model. Dotted curve: goethite component estimated by DC extraction. Dashed curves: ferrinol- or aluminol-like sites estimated by strong acid extraction of quartz grains and with an assumed site density of  $0.2\text{ mol of sites/mol of Fe or Al}$ . Solid curve: ferrinol- and aluminol-like sites with an assumed site density of  $0.2\text{ mol of sites/mol of Fe or Al}$ .

covered to a large extent with a coating rich in Fe and Al, with very little Mn present (17, 32). These elements were probably derived from the weathering of feldspars and Fe-bearing minerals present in the sediment. It is not known whether the coating is predominantly a silicate, an oxyhydroxide, or a hydrotalcite-like, layered double hydroxide (67). The coating was resistant to the 30-min hydroxylamine hydrochloric acid (HH) extraction that is commonly used to dissolve noncrystalline hydrous iron oxides (68), and TEM characterizations of the coating suggested that polycrystalline and single mineral crystalline phases were present (17).

On the basis of this evidence, different CA models were formulated based on the abundance of Fe and Al functional groups at the sediment surface determined by various types of aqueous extractions. Ferrihydrite abundance at the surface was estimated at  $0.9\text{ }\mu\text{mol of Fe/g of sediment}$  from a 30-min HH extraction (17). Adsorption of  $\text{Zn}^{2+}$  by the ferrihydrite in the sediment was simulated using the DDL model of Dzombak and Morel (20). It was assumed that Fe dissolved by the extraction was derived from ferrihydrite with the same density of strong and weak binding sites assigned in the model (20) and that the DDL model calibrated with pure ferrihydrite was valid for ferrihydrite present as a coating on the sediment. The model simulation (Figure 6) suggests that ferrihydrite was not present in sufficient abundance to have an appreciable effect on the measured  $\text{Zn}^{2+}$  adsorption by the Cape Cod sediment. This finding agrees with the experimental observation that a 30-min HH extraction of the sediment did not have an appreciable effect on  $\text{Zn}^{2+}$  adsorption (17).

Since ferrihydrite is apparently not present in sufficient abundance to explain  $\text{Zn}^{2+}$  adsorption, stronger extractions were performed to quantify the Fe and Al present in surface coatings. A 24-h dithionite-citrate-ammonium (DC) extraction, designed to dissolve crystalline iron oxide phases such as goethite and hematite (68), dissolved  $11\text{ }\mu\text{mol of Fe/g of sediment}$ . To estimate the abundance of Fe and Al present in quartz grain coatings, a quartz mineral fraction was separated from the composite sediment sample (17) and leached with  $4\text{ M HCl}$  at  $100\text{ }^\circ\text{C}$  for 8 h. This extraction

yielded  $8\text{ }\mu\text{mol of Fe}$  and  $17\text{ }\mu\text{mol of Al/g of quartz}$ . Zachara et al. (9) also observed that mineral coatings contained greater abundances of extractable Al than Fe in subsurface sediments. Isolation of the separate quartz mineral fraction was critical to the determination of Fe and Al present as coatings on quartz grains. Without this preparative step, the strong extractions required to dissolve the coating also dissolved discrete grains of feldspars, magnetite, hematite, and other magnetically susceptible mineral phases, leading to an overestimate of the Fe and Al present in grain coatings.

**Apparent Binding Constants for  $\text{Zn}^{2+}$  Complexation with Aluminol and Ferrinol Groups.** Stability constants for  $\text{Zn}^{2+}$  adsorption by goethite, hematite, ferrihydrite, and poorly crystalline alumina were determined by fitting experimental data from the literature (38, 69–71). Apparent stability constants for SC models are always model- and parameter-dependent, and thus it is necessary to use a self-consistent model to derive the apparent stability constants (5). Because of the excellent fit between the experimental data and the NEM models above and the difficulty in applying correct electrostatic correction terms to the mass action equations for the sediment, we determined apparent stability constants for the NEM for adsorption of  $\text{Zn}^{2+}$  on goethite, hematite, and poorly crystalline alumina (Table 2). The constants were determined by fitting the experimental data with the one site-one proton NEM; the two site NEM could not be used for fitting these experimental data because  $\text{Zn}^{2+}$  adsorption was not measured as a function of Zn concentration.

To test the importance of the crystalline iron oxide phases, Fe dissolved in the DC extraction was used to estimate the abundance of goethite or hematite phases present. To calculate a site density, it was assumed that these phases had a surface area of  $50\text{ m}^2/\text{g FeOOH}$ , which is a typical specific surface area for laboratory preparations of goethite particles with particle dimensions on the order of  $0.1\text{--}0.2\text{ }\mu\text{m}$ . One site model simulations were performed assuming that either goethite or hematite dominated  $\text{Zn}^{2+}$  adsorption by the sediment and using the apparent stability constants derived for these mineral phases (Table 2). The calculations for goethite are shown in Figure 6; the results suggest that goethite surface hydroxyls were not present in sufficient abundance to explain  $\text{Zn}^{2+}$  adsorption by the sediment. A similar result was obtained assuming that all Fe dissolved was present as hematite (simulations not shown).

**Surface Area of Grain Coatings.** Although the surface coating on the quartz grains appears to have crystalline properties, its thickness over most of the surface is within the range of  $10\text{--}300\text{ nm}$  (17). TEM results indicate the presence of particles with diameters less than  $10\text{ nm}$ , and the surface-to-volume ratios of such particles are much greater than would be the case for goethite particles in the  $0.1\text{--}0.2\text{ }\mu\text{m}$  size range. It is estimated that  $\equiv\text{FeOH}$  at the surface of ferrihydrite represents approximately 20% or more of the total Fe in the particles, which are on the order of a few nanometers in length (20, 72, 73). In contrast, Fe atoms at the surface of goethite particles (with a surface area of  $50\text{ m}^2/\text{g}$ ) are only about 1.7% of the total Fe. Thus,  $\equiv\text{FeOH}$  surface site density in the coatings on the Cape Cod sediment sample could be much greater than was assumed in the goethite model simulations shown in Figure 6.

If it is assumed that Fe and Al dissolved in the  $4\text{ M HCl}$  extraction of the quartz fraction are derived from mineral phases with a surface:bulk Fe (or Al) molar ratio similar to ferrihydrite, then the site density used in CA model simulations would be considerably larger. Figure 6 shows the results of one site NEM simulations assuming that 20% of the extracted Fe or Al was originally present as  $\equiv\text{FeOH}$  or  $\equiv\text{AlOH}$  surface sites. The apparent stability constants for  $\text{Zn}^{2+}$  adsorption reactions with these surface sites were derived from laboratory studies of poorly crystalline alumina

and ferrihydrite (Table 2). The individual model calculations for each site type ( $\equiv\text{FeOH}$  and  $\equiv\text{AlOH}$ ) are much closer to simulating the  $\text{Zn}^{2+}$  reactivity with the Cape Cod sediment surface (Figure 6). An NEM model simulation with both site types present (shown as the  $\equiv\text{FeOH} + \equiv\text{AlO}$  curve in Figure 6) passes through the experimental data. Thus, if the phases present in the quartz grain coatings have a surface area and site density similar to poorly crystalline phases, then the CA modeling approach provides an excellent prediction of  $\text{Zn}^{2+}$  adsorption by the Cape Cod sediment (Figure 6).

The results above are encouraging but also raise several questions. The assumption that the coating has a site density similar to ferrihydrite was arbitrary; is this a reasonable assumption for the Cape Cod sediment or for other soil and sediment samples? To achieve the site densities of  $\equiv\text{FeOH}$  and  $\equiv\text{AlOH}$  used in the model simulations above requires a surface coating 5–20 atomic layers thick (depending on the surface area assumed for the coating), in reasonable agreement with the TOF–SIMS results (17). However, the structure of the coating must be open or porous, so that a significant percentage of Fe and Al in the coating is available for SC reactions with  $\text{Zn}^{2+}$ . This could occur if the coating formed by an accumulation of aggregated small particles or by multilayer sorption of polymeric oxyhydroxides of Fe and Al. But if the structure of the coating is open, then why is it not more easily dissolved by the 30-min HH extraction commonly used to dissolve noncrystalline material? Perhaps the precipitation of silicate-bearing minerals or layered mixed metal hydroxides renders the coating less soluble in short-term HH extractions, or perhaps the 0.5-h extraction time is not sufficient to dissolve noncrystalline deposits located within a network of intergranular pores.

### Comparison of Modeling Approaches

Although the GC approach was successful in simulating  $\text{Zn}^{2+}$  adsorption data, a disadvantage of this approach is that it does not utilize conclusions about actual surface speciation that may be determined from spectroscopic methods. On the other hand, recent advances indicate that earlier SC modeling approaches also have oversimplified the molecular structure of surface complexes and proton stoichiometry of SC equilibria, by using structurally undefined, average surface functional groups (57, 58, 74). In the GC modeling approach, the mass action equations and associated stability constants are valid only for the specific mineral assemblage studied and are not transferable to other mineral assemblages. However, in the authors' opinion, the GC approach is far preferable to empirical approaches, such as distribution coefficients ( $K_d$ ) and adsorption isotherms, because the important linkage between surface and aqueous species is retained in the modeling through the coupling of mass action equations (28). With only three adjustable parameters, the two site NEM model can describe the variation in  $\text{Zn}^{2+}$  adsorption as a function of pH and  $\text{Zn}_T$  concentration within the Cape Cod aquifer; these variations are equivalent to a 3 order of magnitude range in  $K_d$  values (Figure 7). In this way, the effects of variations in pH and aqueous complexation on  $\text{Zn}^{2+}$  adsorption may be simulated equally well as in the CA modeling approach. In addition, the number of surface equilibria that must be considered can be minimized, which is an important practical consideration when coupling SC models within larger solute transport or nuclear waste repository performance assessment models (62, 75, 76).

The results with both modeling approaches indicate that the SC concept can be applied to model ion adsorption by soils and sediments and that an SC model without electrostatic correction terms can be useful for that purpose. The GC approach requires less information and laboratory data and is likely more useful for immediate and practical applications. The CA approach can be applied when the

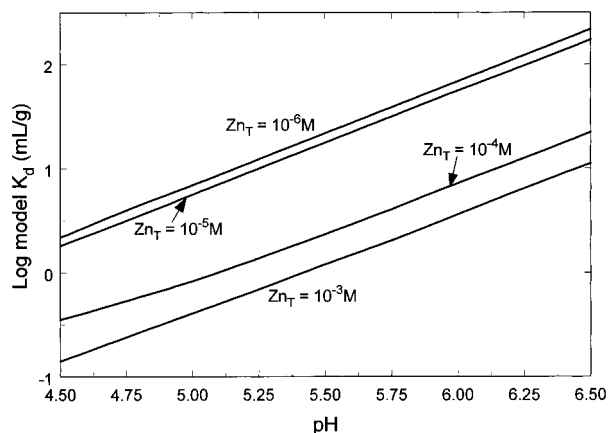


FIGURE 7. Calculated values of the distribution coefficient ( $K_d$ ) for adsorption of  $\text{Zn}^{2+}$  as a function of pH and total  $\text{Zn(II)}$  concentration per liter of water in the Cape Cod aquifer using the two site–one proton model. Solid:water ratio in the aquifer is 4.145 kg of sediment/L of water with an estimated surface area of 0.3  $\text{m}^2/\text{g}$  (32). Strong site concentration in the aquifer is  $4.1 \times 10^{-5}$  mol/L; weak site concentration is  $4.7 \times 10^{-3}$  mol/L.

mineral surface composition is well understood, but even in these cases, some assumptions and parameter values may need to be adjusted to achieve satisfactory results. The challenge in improving the CA approach appears to be better characterization of the composition of sediments surface coatings at the molecular level, including more research on the utility of specialized aqueous extractions as a means of quantifying surface functional groups.

### Acknowledgments

The authors thank J. Bargar, P. Glynn, G. Waychunas, and three anonymous reviewers for their useful suggestions. The research in this paper has been funded in part by the U.S. Environmental Protection Agency (Interagency Agreement DW14935626), but it has not been subjected to the Agency's peer and administrative review and therefore may not necessarily reflect the views of the Agency. The research was also funded in part by the U.S. Geological Survey Toxic Substances Hydrology program.

### Literature Cited

- 1) J. Stumm, W.; Huang, C. P.; Jenkins, S. R. *Croat. Chem. Acta* **1970**, *42*, 223–244.
- 2) Schindler, P. W.; Kamber, H. R. *Helv. Chim. Acta* **1968**, *51*, 1781–1786.
- 3) Schindler, P. W.; Gamsjager, H. *Kolloid Z. Z. Polym.* **1972**, *250*, 759–763.
- 4) Hohl, H.; Stumm, W. *J. Colloid Interface Sci.* **1976**, *55*, 281–288.
- 5) Davis, J. A.; Kent, D. B. In *Mineral–Water Interface Geochemistry*; Hochella, M. F., White, A. F., Eds.; Reviews in Mineralogy, Vol. 23; Mineralogical Society of America: Washington, DC, 1990; pp 177–260.
- 6) Sposito, G. *J. Colloid Interface Sci.* **1983**, *91*, 329–340.
- 7) Turner, G. D.; Zachara, J. M.; McKinley, J. P.; Smith, S. C. *Geochim. Cosmochim. Acta* **1996**, *60*, 3399–3414.
- 8) Zachara, J. M.; Gassman, P. L.; Smith, S. C.; Taylor, D. *Geochim. Cosmochim. Acta* **1995**, *59*, 4449–4464.
- 9) Zachara, J. M.; Smith, S. C.; Kuzel, L. S. *Geochim. Cosmochim. Acta* **1995**, *59*, 4825–4844.
- 10) Zachara, J. M.; Resch, C. T.; Smith, S. C. *Geochim. Cosmochim. Acta* **1994**, *58*, 553–566.
- 11) Zachara, J. M.; Smith, S. C.; Cowan, C. E.; Resch, C. T. *Soil Sci. Soc. Am. J.* **1992**, *56*, 1074–1084.
- 12) Wen, X.; Du, Q.; Tang, H. *Environ. Sci. Technol.* **1998**, *32*, 870–875.
- 13) Stollenwerk, K. G. *Water Resour. Res.* **1995**, *31*, 347–357.
- 14) Goldberg, S.; Sposito, G. *Soil Sci. Soc. Am. J.* **1984**, *48*, 779–783.
- 15) Padmanabhan, E.; Mermut, A. R. *Clays Clay Miner.* **1996**, *40*, 675–681.



- (16) Prieve, D. C.; Ruckenstein, E. J. *Colloid Interface Sci.* **1978**, *63*, 317–329.
- (17) Coston, J. A.; Fuller, C. C.; Davis, J. A. *Geochim. Cosmochim. Acta* **1995**, *59*, 3535–3548.
- (18) Davis, J. A.; Gloor, R. *Environ. Sci. Technol.* **1981**, *15*, 1223–1229.
- (19) Wiese, G. R.; Healy, T. W. *J. Colloid Interface Sci.* **1975**, *52*, 452–458.
- (20) Dzombak, D. A.; Morel, F. M. M. *Surface Complexation Modeling: Hydrous Ferric Oxide*; John Wiley: New York, 1990.
- (21) Davis, J. A.; James, R. O.; Leckie, J. O. *J. Colloid Interface Sci.* **1978**, *63*, 480–499.
- (22) Bolt, G. H.; van Riemsdijk, W. H. *Aquatic Surface Chemistry*; Stumm, W., Ed.; Wiley: New York, 1987; pp 127–164.
- (23) Cowan, C. E.; Zachara, J. M.; Smith, S. C.; Resch, C. T. *Soil Sci. Soc. Am. J.* **1992**, *56*, 1084–1094.
- (24) Mouvet, C.; Bourg, A. C. M. *Water Res.* **1983**, *17*, 641–649.
- (25) Honeyman, B. D. Ph.D. Thesis, Stanford University, Stanford, CA, 1984.
- (26) Altmann, S. A. Ph.D. Thesis, Stanford University, Stanford, CA, 1984.
- (27) Turner, D. A. *Uniform Approach to Surface Complexation Modeling of Radionuclide Sorption*; CNWRA Report 95-001; Center for Nuclear Waste Regulatory Analyses: San Antonio, TX, 1995.
- (28) Westall, J. C.; Jones, J. D.; Turner, G. D.; Zachara, J. M. *Environ. Sci. Technol.* **1995**, *29*, 951–959.
- (29) Koss, V. *Radiochim. Acta* **1988**, *44/45*, 403–406.
- (30) LeBlanc, D. R.; Garabedian, S. P.; Hess, K. M.; Gelhar, L. W.; Quadri, R. D.; Stollenwerk, K. G.; Wood, W. W. *Water Resour. Res.* **1991**, *27*, 895–910.
- (31) Barber, L. B.; Thurman, E. M.; Runnells, D. J. *Contam. Hydrol.* **1992**, *9*, 35–54.
- (32) Fuller, C. C.; Davis, J. A.; Coston, J. A.; Dixon, E. J. *Contam. Hydrol.* **1996**, *22*, 165–187.
- (33) Kent, D. B.; Davis, J. A.; Anderson, L. C. D.; Rea, B. A.; Waite, T. D. *Water Resour. Res.* **1994**, *30*, 1099–1114.
- (34) Nowack, B.; Sigg, L. *Geochim. Cosmochim. Acta* **1997**, *61*, 951–963.
- (35) Davis, J. A.; Hess, K. M.; Kent, D. B.; Coston, J. A.; Joye, J. L.; Brien, P.; Bussey, K. W. *Multispecies Reactive Tracer Test in a Sand and Gravel Aquifer, Cape Cod, Massachusetts*; EPA Environmental Research Brief; Environmental Protection Agency: Ada, OK, in press.
- (36) Rea, B. A.; Kent, D. B.; LeBlanc, D. R.; Davis, J. A. in *USGS Toxic Substances Hydrology Procedures*; WRIR 91–4034; USGS: Denver, 1991; pp 88–95.
- (37) Papelis, C.; Hayes, K. F.; Leckie, J. O. Technology Report 306, Department of Civil Engineering, Stanford University, 1988.
- (38) Benjamin, M. M.; Leckie, J. O. *J. Colloid Interface Sci.* **1981**, *79*, 209–221.
- (39) Honeyman, B. D.; Leckie, J. O. *Geochemical Processes at Mineral Surfaces*; Davis, J. A., Hayes, K. F., Eds.; ACS Symposium Series 323; American Chemical Society: Washington, DC, 1986; pp 162–190.
- (40) Tessier, A.; Carignan, R.; Dubreuil, B.; Rapin, F. *Geochim. Cosmochim. Acta* **1989**, *53*, 1511–1522.
- (41) Hiebert, F. Z.; Bennett, P. C. *Science* **1992**, *258*, 278–281.
- (42) Parfitt, R. L.; Van der Gaast, S. J.; Childs, C. W. *Clays Clay Miner.* **1992**, *40*, 675–681.
- (43) Jackson, R. E.; Inch, K. J. *J. Contam. Hydrol.* **1989**, *4*, 27–50.
- (44) Davis, J. A. *Geochim. Cosmochim. Acta* **1984**, *48*, 679–691.
- (45) Lovgren, L.; Sjoberg, S.; Schindler, P. W. *Geochim. Cosmochim. Acta* **1990**, *54*, 1301–1306.
- (46) Ainsworth, C. C.; Girvin, D. C.; Zachara, J. M.; Smith, S. C. *Soil Sci. Soc. Am. J.* **1989**, *53*, 411–418.
- (47) O'Day, P. A.; Brown, G. E.; Parks, G. A. *J. Colloid Interface Sci.* **1994**, *165*, 269–289.
- (48) Yates, D. E.; James, R. O.; Healy, T. W. *J. Chem. Soc., Faraday Trans. 1* **1980**, *76*, 1–8.
- (49) Zachara, J. M.; Smith, S. C. *Soil Sci. Soc. Am. J.* **1994**, *58*, 762–769.
- (50) McKinley, J. P.; Zachara, J. M.; Smith, S. C.; Turner, G. D. *Clays Clay Miner.* **1995**, *43*, 586–598.
- (51) Davis, J. A.; Leckie, J. O. *J. Colloid Interface Sci.* **1978**, *67*, 90–107.
- (52) Kinniburgh, D. G. *J. Soil Sci.* **1983**, *34*, 759–768.
- (53) Kurbatov, M. H.; Wood, G. B.; Kurbatov, J. D. *J. Phys. Chem.* **1951**, *55*, 1170–1182.
- (54) Bradbury, M. H.; Baeyens, B. *J. Contam. Hydrol.* **1997**, *27*, 223–248.
- (55) Fuerstenau, D. W.; Manmohan, D.; Raghavan, S. *Adsorption from Aqueous Solutions*; Tewari, P. H., Ed.; Plenum Press: New York, 1981; pp 93–117.
- (56) Charlet, L.; Sposito, G. *Soil Sci. Soc. Am. J.* **1989**, *53*, 691–695.
- (57) Bargar, J. R.; Brown, G. E.; Parks, G. A. *Geochim. Cosmochim. Acta* **1997**, *61*, 2617–2637.
- (58) Bargar, J. R.; Brown, G. E.; Parks, G. A. *Geochim. Cosmochim. Acta* **1997**, *61*, 2639–2652.
- (59) Herbelin, A. L.; Westall, J. C. *FITEQL, A Computer Program for Determination of Chemical Equilibrium Constants from Experimental Data*, ver. 3.1; Department of Chemistry, Oregon State University: 1994.
- (60) Kinniburgh, D. G. *Environ. Sci. Technol.* **1986**, *20*, 895–904.
- (61) Waite, T. D.; Davis, J. A.; Payne, T. E.; Waychunas, G. A.; Xu, N. *Geochim. Cosmochim. Acta* **1994**, *58*, 5465–5478.
- (62) Altmann, S.; Chupeau, J. J. *Contam. Hydrol.* **1997**, *26*, 325–338.
- (63) Belzile, N.; Tessier, A. *Geochim. Cosmochim. Acta* **1990**, *54*, 103–110.
- (64) Fuller, C. C.; Davis, J. A. *Geochim. Cosmochim. Acta* **1987**, *51*, 1491–1502.
- (65) Davis, J. A.; Fuller, C. C.; Cook, A. D. *Geochim. Cosmochim. Acta* **1987**, *51*, 1477–1490.
- (66) Zachara, J. M.; Ainsworth, C. C.; Cowan, C. E.; Resch, C. T. *Soil Sci. Soc. Am. J.* **1989**, *53*, 418–428.
- (67) Scheidegger, A. M.; Lamble, G. M.; Sparks, D. L. *J. Colloid Interface Sci.* **1997**, *186*, 118–128.
- (68) Chao, T. T.; Zhou, L. *Soil Sci. Soc. Am. J.* **1983**, *47*, 225–232.
- (69) McKenzie, R. M. *Aust. J. Soil Res.* **1980**, *18*, 61–73.
- (70) Kinniburgh, D. G.; Jackson, M. L. In *Adsorption of Inorganics at Solid–Liquid Interfaces*; Anderson, M. A., Rubin, A. J., Eds.; Ann Arbor Science: Ann Arbor, MI, 1981; pp 91–160.
- (71) Dempsey, B. A.; Singer, P. C. In *Contaminants and Sediments*; Baker, R. A., Ed.; Ann Arbor Science: Ann Arbor, MI, 1980; Vol. 2, pp 333–352.
- (72) Rea, B. A.; Davis, J. A.; Waychunas, G. A. *Clays Clay Miner.* **1994**, *42*, 23–34.
- (73) Waychunas, G. A.; Rea, B. A.; Fuller, C. C.; Davis, J. A. *Geochim. Cosmochim. Acta* **1993**, *57*, 2251–2269.
- (74) Bargar, J. R.; Towle, S. N.; Brown, G. E.; Parks, G. A. *J. Colloid Interface Sci.* **1997**, *185*, 473–492.
- (75) Yeh, G. T.; Tripathi, V. S. *Water Resour. Res.* **1991**, *27*, 3075–3094.
- (76) Kohler, M.; Curtis, G. P.; Kent, D. B.; Davis, J. A. *Water Resour. Res.* **1996**, *32*, 3539–3551.
- (77) McBride, M. B. *Clays Clay Miner.* **1982**, *30*, 21–28.

Received for review March 27, 1998. Revised manuscript received June 1, 1998. Accepted June 15, 1998.

ES980312Q